

Accepted Manuscript

Noninvasive renal sympathetic denervation by extracorporeal high-intensity focused ultrasound in a preclinical canine model

Qifeng Wang, Rui Guo, Shunkang Rong, Gang Yang, Que Zhu, Yonghong Jiang, Changming Deng, Dichuan Liu, Qi Zhou, Qi Wu, Shunhe Wang, Jun Qian, Qi Wang, Han Lei, Tong-Chuan He, Zhibiao Wang, Jing Huang



PII: S0735-1097(13)01205-9
DOI: 10.1016/j.jacc.2013.02.050
Reference: JAC 18704

To appear in: *Journal of the American College of Cardiology*
Accepted date: 14 February 2013

Please cite this article as: Wang, Q., Guo, R., Rong, S., Yang, G., Zhu, Q., Jiang, Y., Deng, C., Liu, D., Zhou, Q., Wu, Q., Wang, S., Qian, J., Wang, Q., Lei, H., He, T.C., Wang, Z., Huang, J., Noninvasive renal sympathetic denervation by extracorporeal high-intensity focused ultrasound in a preclinical canine model, *Journal of the American College of Cardiology* (2013), doi: 10.1016/j.jacc.2013.02.050.

This is a PDF file of an unedited manuscript that has been accepted for publication. As a service to our customers we are providing this early version of the manuscript. The manuscript will undergo copyediting, typesetting, and review of the resulting proof before it is published in its final form. Please note that during the production process errors may be discovered which could affect the content, and all legal disclaimers that apply to the journal pertain.

Noninvasive renal sympathetic denervation by extracorporeal high-intensity focused ultrasound in a preclinical canine model

Qifeng Wang, MM*; Rui Guo, MD, PhD*; Shunkang Rong, MD*; Gang Yang, MD, PhD; Que Zhu, MD, PhD; Yonghong Jiang, MD; Changming Deng, MD; Dichuan Liu, MD; Qi Zhou, MD, PhD; Qi Wu, MD, PhD; Shunhe Wang, MD; Jun Qian, MM; Qi Wang, MS; Han Lei, MD; Tong-Chuan He, MD, PhD; Zhibiao Wang, MD, PhD and Jing Huang, MD

The Second Affiliated Hospital of Chongqing Medical University (Qif. W., S. R., G. Y., Q. Zhu, Y.J., C.D., D.L., Q. Zhou, Q. Wu, J.Q., J. H.), Chongqing, China; State Key Laboratory of Ultrasound Engineering in Medicine Co-Founded by Chongqing and the Ministry of Science and Technology, and National Engineering Research Center of Ultrasound Medicine (Z.Q., S.R., Q. Wang, Z. Wang., J.H.), Chongqing, China; The First Affiliated Hospital of Chongqing Medical University (R.G., H.L.), Chongqing, China; Chongqing Medical University (S.W.), Chongqing, China; Molecular Oncology Laboratory, Department of Surgery, The University of Chicago Medical Center (T-C. He.), Chicago, IL, USA. *The first 3 authors contribute equally and are joint first authors to this article.

Brief title: Noninvasive RSD by extracorporeal HIFU

Word count: 3869

Funding:

This study was supported in part by research grants from the National Natural Science Foundation of China (30527001, 30830040, 81201173), the National Key Basic Research Program (973 Program, 2011CB707902), and the Foundation for Key Scientific and Technical Research of Chongqing, China (CSTC2005AA5008-5, CSTC2009AB5003).

Relationship with industry:

Zhibiao Wang is a shareholder in and full-time employee of Chongqing Haifu, Chongqing, China. However, other authors have no conflicts of interest.

Reprint requests and correspondence:

Prof. Jing Huang, MD
Professor and Vice Chair, Department of Cardiology
The Second Affiliated Hospital, Chongqing Medical University
Chongqing 400010, China
Fax: +8602363711527; Tel: +8613508312022
E-mail: huangjing@cqmu.edu.cn; huangjing_9901@yahoo.com.

Acknowledgments: We thank Dr. Rong Jiang, for histological analysis assistance, Prof. Gengbiao Yuan, for NA detection assistance, and Prof. Xiaoni Zhong, for statistical analysis assistance, and they are all from Chongqing Medical University.

Abstract**Objectives**

The feasibility of noninvasive renal sympathetic denervation (RSD) using the novel approach of extracorporeal high-intensity focused ultrasound (HIFU) was investigated in this study.

Background

Catheter-based RSD has achieved promising clinical outcomes.

Methods

Under the guidance of Doppler flow imaging, therapeutic ablations (250 W×2 seconds) were performed by extracorporeal HIFU on the bilateral renal nerves (36.3 ± 2.8 HIFU emissions in each animal) in an average 27.4-minute procedure in 18 healthy canines of the ablation group. Similar procedures without acoustic energy treatment were conducted in 5 canines of the sham group. The animals were sacrificed on day 6 or 28. The blood pressure (BP), plasma noradrenaline (NA) level and renal function were determined on days 0, 6 and 28. Pathological examinations were performed on all retrieved samples.

Results

All of the animals survived the treatment. After ablation, the BP and NA significantly decreased compared to the baseline values (Bp changed $-15.9/-13.6$ mmHg, NA changed -55.4% , $p < 0.001$, respectively, on 28 days after ablation) and compared to the sham group on days 6 and 28. Ablation lesions around the renal artery adventitia were observed on day 6. A histologic examination revealed the disruption of nerve fibers, necrosis of Schwann cells and neurons, and apparent denervation on day 28. No procedure-related complications were observed.

Conclusions

Effective RSD was successfully achieved using the extracorporeal HIFU method in canines. Thus, noninvasive HIFU may be further explored as an important and novel strategy for RSD.

Key words: Extracorporeal high-intensity focused ultrasound, Renal sympathetic denervation, Noninvasive, Hypertension, Ablation

Abbreviations

HIFU=High-intensity focused ultrasound

RSD=Renal sympathetic denervation

CDFI=Color Doppler flowing imaging

NA=Noradrenaline

BUN=Urea nitrogen

sCr=Serum creatinine

Na⁺=Sodium

BP=Blood pressure

SBP=Systolic blood pressure

DBP=Diastolic blood pressure

Introduction

It is estimated that one billion individuals worldwide suffer from hypertension, and hypertension-related complications are recognized as the major cause of morbidity and mortality (1). Recently, a catheter-based strategy for renal sympathetic denervation (RSD) has been developed for the management of drug-resistant hypertension and has achieved encouraging clinical outcomes (2). The therapeutic benefits of RSD have also been shown for those diseases associated with sympathetic overactivity, such as insulin resistance, arrhythmia, and heart failure (3,4). However, intervention-related complications can occasionally occur. In addition, vascular wall injury has been observed in a preclinical model (5), and hemodynamic stenosis has been found in clinical case reports due to possibly related complications (6). Recently, many new devices are under-investigation, such as chemical renal denervation using a drug delivery approach by a sidehole balloon catheter, which may help to reduce the potential damage to the artery wall (7).

High-intensity focused ultrasound (HIFU) has been used to noninvasively ablate tissue by extracorporeally delivering focused acoustic energy. This technique is considered the ideal source of energy, especially for the ablation of deep solid tissue (8). It has also been clinically used to treat uterus, kidney and liver tumors (9,10). In addition, the application of HIFU has been expanded significantly in recent years (11,12).

To the best of our knowledge, few studies have reported the use of noninvasive HIFU for RSD. This study was designed to explore the possible use of this new technique for RSD in a canine model by investigating the feasibility and safety associated with this procedure.

Methods

HIFU System for RSD

The HIFU tumor therapeutic system (Model-JC200, certified by the European Union, Chongqing Haifu Technology Co. Ltd., China) was used. The therapeutic focused ultrasound beam was produced by a 220 mm spherically curved therapeutic transducer with focal length of 132 mm. The physical focal region was ellipsoid and less than $2 \times 2 \times 6 \text{ mm}^3$. The operating frequency was 0.98 MHz (corresponding to 1.58 mm wavelength). The acoustic power of the therapeutic transducer ranged from 33 W to 550 W, with an acoustic intensity at focus from 467 W/cm^2 to 7785 W/cm^2 under a degassed water acoustic environment. A diagnostic probe was aligned coaxially to the therapeutic transducer to locate the target tissues. By adjusting the transducer in three dimensions, the focus could be moved 1 mm by 1 mm to target at the renal artery.

Animal Preparation

The experimental protocol was approved by the Institutional Ethics Committee of Chongqing Medical University. The use and care of the animals were in compliance with the US National Institutes of Health Guide for Care and Use of Laboratory Animals.

Twenty-three healthy mongrel canines (15 to 20 kg, purchased through the Experimental Animal Care Center of Chongqing Medical University) of either sex were distributed randomly into an ablation group (N=18) and a sham group (N=5). All of the canines were anesthetized with 3% pentobarbital sodium (30 mg/kg) intraperitoneally. The abdominal fur along the acoustic path was removed, and the skin was degreased with 75% alcohol and suctioned for degassing. The

right femoral artery was punctured, and a syringe attached to a pressotransducer (Model YPJ01, Chengdu Instrument Factory, Chengdu, China) temporarily for every invasive blood pressure (BP) measurements. The BP was recorded with a RM6240 Physiology Signal Collection Processing System (Chengdu Instrument Factory, Chengdu, China) prior to ablation (defined as baseline). At days 6 and 28 post ablation, the follow-up study used a similar procedure to measure the blood pressure. Every BP was recorded at 30 minutes post anesthesia.

HIFU Ablation Procedure for RSD

In the ablation group, the left abdominal wall of each canine was immersed in the therapeutic chamber filled with degassed water, which provided acoustic coupling between the transducer and skin (13). Color Doppler flowing imaging (CDFI) on the long-axis view of the left renal artery was obtained by adjusting the relative positions of the transducer and animal (Fig. 1A). Using CDFI as a guide, the foci of the extracorporeal HIFU were set on zygomorphic wall at the proximal, middle and distal right renal artery, respectively. Therapeutic ablations ($250\text{ W}\times 2\text{ s}$) were performed at each set of foci. A total of 6 emissions of acoustic power were delivered when every segment of the renal artery was visible on an ultrasonographic view (Fig. 1B). The therapeutic transducer was moved 2 mm dorsally or ventrally to initiate the viewing of the next set of ablations. In each visual field, the focus locations and power emissions were guided by CDFI. For example, there were two emissions of acoustic delivery if the ultrasonographic view could only provide the proximal segment, and the deliveries of acoustic energy were not finished until the CDFI of the renal artery disappeared. The same procedure was subsequently performed on the right renal artery. In the sham group, 5 canines underwent a similar procedure without the

delivery of acoustic energy. The procedure time, defined as the duration when the animal was immersed in the therapeutic chamber until the bilateral renal nerve had been ablated, was recorded for every animals.

Post-Ablation Procedure

All animals received standard care. In the ablation group, the canines were euthanatized on day 6 (N=10) or day 28 (N=8) post-ablation by intravenous injection of 10% potassium chloride after the BP was measured invasively. The tissues along the acoustic path and near the foci, including the abdominal wall, kidney, spleen, ureters, intestinal tract, liver and target renal artery, were retrieved for gross and histological examination. In the sham group, the BP was also measured on days 6 and 28, and the histological examination was performed on day 28.

Renal Function and Sympathetic Activity Detection

The plasma noradrenaline (NA) concentration was measured by a commercially available radioimmunoassay kit (Labor Diagnostika Nord GmbH & Co. KG, Germany) (14). Urea nitrogen (BUN), serum creatinine (sCr) and serum sodium (Na^+) were measured using a standard procedure prior to ablation and on days 6 and 28.

Statistical Analysis

Changes in BP, NA, BUN, sCr and Na^+ values were analyzed from baseline to 6 or 28 days by ANOVAs for completely randomized and for repeated measure designs. $p < 0.05$ was considered statistically significant. The data are presented as the mean \pm standard deviation or percent change (%). All statistical analyses were performed with SAS software for Windows (SAS 9.3 Institute Inc, Cary, NC, USA).

Results

Overall Procedural Considerations

CDFI of the targeted renal artery was acquired in all experimental canines. In this study, 3 to 5 CDFI-guided ultrasonographic views of the renal arteries were obtained in each unilateral renal artery, although some views only showed segmental vessels. The total HIFU ablation was 36.3 ± 2.8 emissions for the RSD of each pair of renal arteries, and the procedure time was 27.4 ± 3.7 minutes.

Blood Pressure Measurement

On days 6 and 28 post-ablation, the SBP (12.3 and 15.9 mm Hg on days 6 and 28, both $p < 0.001$) and DBP (11.6 and 13.6 mm Hg on days 6 and 28, both $p < 0.001$) significantly decreased relative to the individual baseline BP (Fig. 2A). Similarly, after ablation, the BP in the ablation group was significantly lower than that of the sham group on both days.

In the sham group, during the baseline, 6 and 28 days follow-up, the BP had not significantly changed (Tab. 1).

Renal Functions and Sympathetic Activity Detection

On day 6 post-ablation, NA was reduced by 50.1% ($p < 0.001$), but BUN, sCr, and Na^+ were not significantly different from the baseline levels. However, both NA (55.4%, $p < 0.001$) and Na^+ (4.5%, $p = 0.007$) were reduced on day 28 post-ablation, while BUN and sCr were not significantly different from baseline (Fig. 2B). Meanwhile, NA and Na^+ in the ablation group were significantly lower than that of the sham group on day 28.

In the sham group, during the baseline, 6 and 28 days follow-up, there were not significantly

different among NA, BUN, sCr, and Na⁺ (Tab. 1).

Gross and Histological Evaluation

In the ablation group, a gross examination showed the presence of several hemorrhagic spots on the fatty tissue around the target renal arteries in a diffused or clustered distribution pattern on day 6. After removing the fatty tissue layer, ablation lesions were also found on the renal artery adventitia, and some lesions were clustered around the nerve fibers (Fig. 3A). On day 28, the slightly yellow fatty tissue was adhered to the target regions, although the lesions of the fatty tissue were gone (Fig. 3B).

A histological evaluation showed the vacuolar change of the target nerve fibers and a change of the interstitium to a mildly myxoid phenotype on day 6. The nuclei of the Schwann cells were darkly stained and exhibited pyknosis or karyorrhexis, or were even absent (Fig. 4A and 4B). The distal regions of the target lesions showed ganglion-like degeneration, swelling of the perikaryon, eosinophilic enrichment and, in some cases, the disappearance of Nissl bodies.

On day 28, the target nerve fibers appeared shrunken and vacuolated. Necrosis of the Schwann cells was also observed around the targeted area. The myxoid change of the nerve fibers was more apparent than on day 6 (Fig. 4C and 4D). In the sham group, the histological findings remained unchanged.

Safety Considerations

The vital signs of all canines were normal during the procedure and post-ablation. All of the canines survived the treatment until they were sacrificed. The gross and histological evaluations did not reveal significant injuries along the acoustic path, including the skin, liver, spleen, kidney,

ureters, intestinal tract, and the tissue around the target region.

The targeted renal arteries were smooth and had an intact vascular wall and endothelium. The ablation lesions were only found on the adventitia and immediately surrounding the fatty tissue. Bleeding spots, ulcers and thrombi were not observed on the targeted renal arteries. In addition, a histological examination showed an intact vascular structure with an intact endothelium and vascular smooth muscle cells. No evidence of inflammatory cell infiltration, hyperplasia or stenosis was observed 28 days later.

Discussion

The HIFU technique is a promising strategy for noninvasive deep-tissue ablation due to its ability to penetrate and target tissues of interest. The acoustic energy can be delivered to the target region inside the body for therapeutic ablation without significant tissue injury along the path of the acoustic beam and with acceptable targeting accuracy in clinic practice (10,15). In this study, noninvasive RSD ablation was achieved in every animal using a clinically approved HIFU apparatus. After properly preparing the skin by degreasing and degassing, the energy can be more effectively delivered into the target tissues, thus reducing the energy loss and possible tissue injury along the acoustic path. On day 28 post-ablation, both BP and NA were significantly lower than the baseline and the sham group. Hyperplasia and stenosis of the renal arteries were not found, while the disruption of the renal nerve still remained, and the myxoid change and shrinkage of renal nerve fibers were more significant, which suggested the renal sympathetic denervation still persisted. The sham group served to control for factors related to HIFU that could interfere with the results. The results from the sham group show that our noninvasive

approach had little impact on BP and NA.

With the guidance of CDFI, extracorporeal HIFU acoustic energy can be easily targeted to the renal artery. In our dual renal nerves ablation, an average of 36.3 acoustic emissions were delivered, but the cumulative duration was only approximately 73 seconds, so the entire procedure duration can be limited to a half-hour in general. Although the size of a single lesion created by HIFU ablation is relatively small, increasing the number of ablations in the renal artery adventitia using different viewing segments should improve the safety and efficiency of RSD.

It remains controversial whether RSD affects the BP of normotensive animals. Some studies indicated that the BP was reduced in comparison to the baseline (16,17). In this study, BP was significantly decreased in a large, healthy, aggressive animal model, which correlated with a remarkable decrease in plasma noradrenaline, suggesting that the sympathetic activity may be at least partially reduced by HIFU ablation. The extent of the decrease in DBP was similar to the decrease in SBP. Interestingly, our results differ from those reported by some previous studies, which showed that the SBP decreased markedly more than the DBP did (2). One possible reason for this difference may be indirectly attributed to the decreased blood volume and sodium levels caused by the large reduction of noradrenaline in our normal-BP model after HIFU ablation. Furthermore, our results suggest that the HIFU-mediated RSD may be permanent because the myxoid change and shrinkage of the targeted renal nerve fibers were still present 28 days post-ablation.

Although HIFU acoustic energy targeted whole layers of the renal arteries, a pathological

evaluation revealed that both the vascular wall and the endothelial layer remained intact. The therapeutically ablated regions were restricted to the vascular adventitia and the area immediately surrounding the fatty tissue. This phenomenon may be explained by the possible cooling effect of the rapidly circulating bloodstream within the targeted renal arteries and the absence of any catheter to limit the flow of the renal artery. This result is consistent with the previous report that blood vessels are more resistant to acoustic energy (18). On the other hand, Ultrasound-inhibited nerve conduction block for pain management and treatment of spasticity has been actively investigated for nearly 50 years, which can be achieved in lower acoustic energy, suggested that the nerve fibers may be more sensitive to HIFU energy (19, 20). While the gross and histological appearance of the nerve fibers around the ablation target area was normal, a pathological examination revealed that the nerve fiber structure was significantly damaged and disrupted after ablation 28 days. Thus, this phenomenon suggests that acoustic energy may selectively target the nerve fibers at a lower acoustic intensity level.

Although the incidence of pain was frequent, the pain was described as slight to moderate in the patients with uterine fibroids undergoing HIFU ablation (21), which the ablative depth was similar to the study. With lower energy intensity and very short duration of acoustic delivery, the authors presumed that the pain experienced by patients using HIFU ablation is acceptable.

High acoustic intensity and long-time acoustic energy delivery may induce skin toxicity (8/30) and edema (8/30) at the treatment site when HIFU was used for tumor ablation, although most of these side effects were slight (10). In this study, the acoustic intensity and exposure were significantly lower than used in previous studies, and the cumulative acoustic energy used in this

study was approximately 3% of that previously used for clinical tumor ablation (i.e. 250 vs. 399.5 W, 72 vs. 1200 s) (10, 21). Additionally, our total procedure time was significantly shorter. Thus, the lower energy input delivered by HIFU may reduce the discomfort and damage caused by the procedure, and this further supports the safety claims of its possible use in RSD in clinical settings.

We found no evidence of significant injuries along the acoustic transmission path, such as in the abdominal wall, kidney and tissues around the target renal arteries, using gross and microscopic examinations. Nonetheless, it is conceivable that mild injuries occurred along the path but quickly healed because the acoustic intensity within these tissues was far lower than that at the focal points.

Unlike the catheter-based strategy, the HIFU-mediated RSD technique can be performed relatively independently of anatomical variations in renal arteries. Thus, this technique may be more suitable for certain conditions, such as bifurcated renal arteries and renal arteries that are smaller and shorter than normal (22). In contrast to the catheter-based strategy, the HIFU technique uses ultrasound without X-irradiation as a guide, which helps avoid radiation damage to both patients and operators. Furthermore, although the therapeutic region of a single ablation is relatively small, multiple ablation points may be combined to achieve a desirable RSD for individual patients. Mild RSD may be more suitable for individuals with common hypertension and is not limited to those with drug-resistant hypertension.

Limitations

An invasive BP measurement under anesthesia instead of in the conscious state was performed

in this study due to the technical difficulties of the latter. We observed a possible change in BP measured in the conscious state following HIFU, which needs further evaluation. The effect of targeting RSD using the HIFU technique depended on the acoustic window and required CDFI guidance. Therefore, this new technique may be not suitable for obese patients or patients with emphysema. As an alternative, it may be possible to use HIFU guided by MRI. Furthermore, a long-term follow-up study is necessary to fully evaluate the efficacy and safety of the HIFU strategy. A clinical trial may provide the most valuable information.

Conclusions

Under CDFI guidance, RSD was achieved in a noninvasive manner in normotensive canines using the extracorporeal HIFU technique without significant morbidity or mortality. Therefore, this new strategy may provide an alternate approach to the clinical treatment of drug-resistant hypertension and other conditions associated with sympathetic overactivity.

References

1. Calhoun DA, Jones D, Textor S, et al. Resistant hypertension: diagnosis, evaluation, and treatment: a scientific statement from the American Heart Association Professional Education Committee of the Council for High Blood Pressure Research. *Circulation* 2008;117:e510-26.
2. Esler MD, Krum H, Sobotka PA, et al. Renal sympathetic denervation in patients with treatment-resistant hypertension (The Symplicity HTN-2 Trial): a randomised controlled trial. *Lancet* 2010;376:1903-9.
3. Ajijola OA, Lellouche N, Bourke T, et al. Bilateral cardiac sympathetic denervation for the management of electrical storm. *J Am Coll Cardiol* 2012;59:91-2.
4. Brandt MC, Mahfoud F, Reda S, et al. Renal sympathetic denervation reduces left ventricular hypertrophy and improves cardiac function in patients with resistant hypertension. *J Am Coll Cardiol* 2012;59:901-9.
5. Rippy MK, Zarins D, Barman NC, et al. Catheter-based renal sympathetic denervation: Chronic preclinical evidence for renal artery safety. *Clin Res Cardiol* 2011;100: 1095-101.
6. Vonend O, Antoch G, Rump LC, et al. Secondary rise in blood pressure after renal denervation. *Lancet* 2012;380:778.
7. Stefanadis C, Toutouzas K, Synetos A, et al. Chemical denervation of the renal artery by vincristine in swine. A new catheter based technique. *Int J Cardiol* 2012 Jan 20 [E-pub ahead of print], doi:10.1016/j.ijcard.2012.01.002.
8. Kennedy JE. High-intensity focused ultrasound in the treatment of solid tumours. *Nat Rev*

- Cancer 2005;5:321-7.
9. Ng KK, Poon RT, Chan SC, et al. High-intensity focused ultrasound for hepatocellular carcinoma: a single-center experience. *Ann Surg* 2011;253:981-7.
 10. Illing RO, Kennedy JE, Wu F, et al. The safety and feasibility of extracorporeal high-intensity focused ultrasound (HIFU) for the treatment of liver and kidney tumours in a Western population. *Br J Cancer* 2005;93:890-5.
 11. Marsac L, Chauvet D, Larrat B, et al. MR-guided adaptive focusing of therapeutic ultrasound beams in the human head. *Med Phys* 2012;39:1141-9.
 12. Aptel F, Charrel T, Lafon C, et al. Miniaturized high-intensity focused ultrasound device in patients with glaucoma: a clinical pilot study. *Invest Ophthalmol Vis Sci* 2011;52:8747-53.
 13. Casarotto RA, Adamowski JC, Fallopa F, et al. Coupling agents in therapeutic ultrasound: acoustic and thermal behavior. *Arch Phys Med Rehabil* 2004;85:162-5.
 14. Watt MJ, Holmes AG, Steinberg GR, et al. Reduced plasma FFA availability increases net triacylglycerol degradation, but not GPAT or HSL activity, in human skeletal muscle. *Am J Physiol Endocrinol Metab* 2004;287:E120-7.
 15. Leslie T, Ritchie R, Illing R, et al. High-intensity focused ultrasound treatment of liver tumours: post-treatment MRI correlates well with intra-operative estimates of treatment volume. *Br J Radiol* 2012;85:1363-70.
 16. Pappas BA, Petersa DAV, Saari M. Neonatal 6-hydroxydopamine sympathectomy in normotensive and spontaneously hypertensive rat. *Pharmacology Biochemistry and Behavior*, 1974;2: 381-6.

-
17. Jacob F, Ariza P, Osborn JW. Renal denervation chronically lowers arterial pressure independent of dietary sodium intake in normal rats. *Am J Physiol Heart Circ Physiol* 2003;284:H2302-10.
 18. Dasgupta S, Banerjee RK, Hariharan P, et al. Beam localization in HIFU temperature measurements using thermocouples, with application to cooling by large blood vessels. *Ultrasonics* 2011;51:171-80.
 19. Foley JL, Little JW, Vaezy S. Effects of high-intensity focused ultrasound on nerve conduction. *Muscle Nerve* 2008;37:241-50.
 20. Foley JL, Little JW, Starr FL, et al. Image-guided HIFU neurolysis of peripheral nerves to treat spasticity and pain. *Ultrasound Med Biol* 2004;30:1199-207.
 21. Zhao WP, Chen JY, Zhang L, et al. Feasibility of ultrasound-guided high intensity focused ultrasound ablating uterine fibroids with hyperintense on T2-weighted MR imaging. *Eur J Radiol* 2012 Sep 20 [E-pub ahead of print], doi: 10.1016/j.ejrad.2012.08.020.
 22. Sapoval M, Azizi M, Bobrie G, et al. Endovascular renal artery denervation: why, when, and how? *Cardiovasc Intervent Radiol* 2012;35:463-71.

Figure legends

Fig. 1A—Schematic of RSD with HIFU - The focus of HIFU energy (green spot) was set to cross the wall of the renal artery. Green spot: the focal point of the HIFU energy; black arrow: renal artery.

Fig. 1B—Ablation foci were set and ablated by CDFI guidance - Ablation foci (green spots) were targeted by 3-dimensional movement of the transducer guided by CDFI. The locations on the renal artery that were ablated appear as red spots. White arrow: kidney; yellow arrow: renal artery.

Fig. 2A—The changes in SBP and DBP on days 6 and 28 after RSD

The BP was significantly lower compared to the baseline values on days 6 and 28 post-ablation in the ablation group, while there was not significant the change of the BP in the sham group.

Fig. 2B—The percent changes in NA, BUN, sCr and Na⁺ on days 6 and 28 after ablation.

In the ablation group, the NA was significantly lower on days 6 and 28, and Na⁺ was lower on day 28 post-ablation compared to the baseline values, respectively. There were not significantly different among NA, BUN, sCr, and Na⁺ at 6 and 28 days follow-up in the sham group.

Fig. 3A—The gross examination of the ablation lesion on day 6 - The ablation lesions (yellow arrows) were also found on the adventitia of renal artery, some lesions clustered around the nerve fibers (green arrows).

Fig. 3B—The gross examination of the ablation lesion on day 28 - The RSD lesions disappeared, and slightly yellow adhered fatty tissue was observed in the proximal, middle and distal regions of the renal artery (yellow arrows).

Fig. 4A—Histologic examination of the target nerve bundles on day 6 after RSD (H&E×100)

- The renal artery with an intact wall and endothelium surrounded by the damaged nerve fibers. The spaces between the perineurium increased due to the edema and pyknosis of renal nerve fibers.

Fig. 4B—Histologic examination of the target nerve bundles on day 6 after RSD (H&E×400)

- The nuclei of Schwann cells are darkly stained and exhibit pyknosis, karyorrhexis or even disappearance. The mild myxoid change of interstitium can be seen.

Fig. 4C—Histologic examination of the target nerve bundles on day 28 after RSD (H&E×100)

- The renal artery with intact wall and endothelium was surrounded by the damaged nerve fibers. The nerve fibers were shrunken and more vacuolated, and the Schwann cells appeared to be more necrotic on day 28 after RSD.

Fig. 4D—Histologic examination of the target nerve bundles on day 28 after RSD (H&E×400)

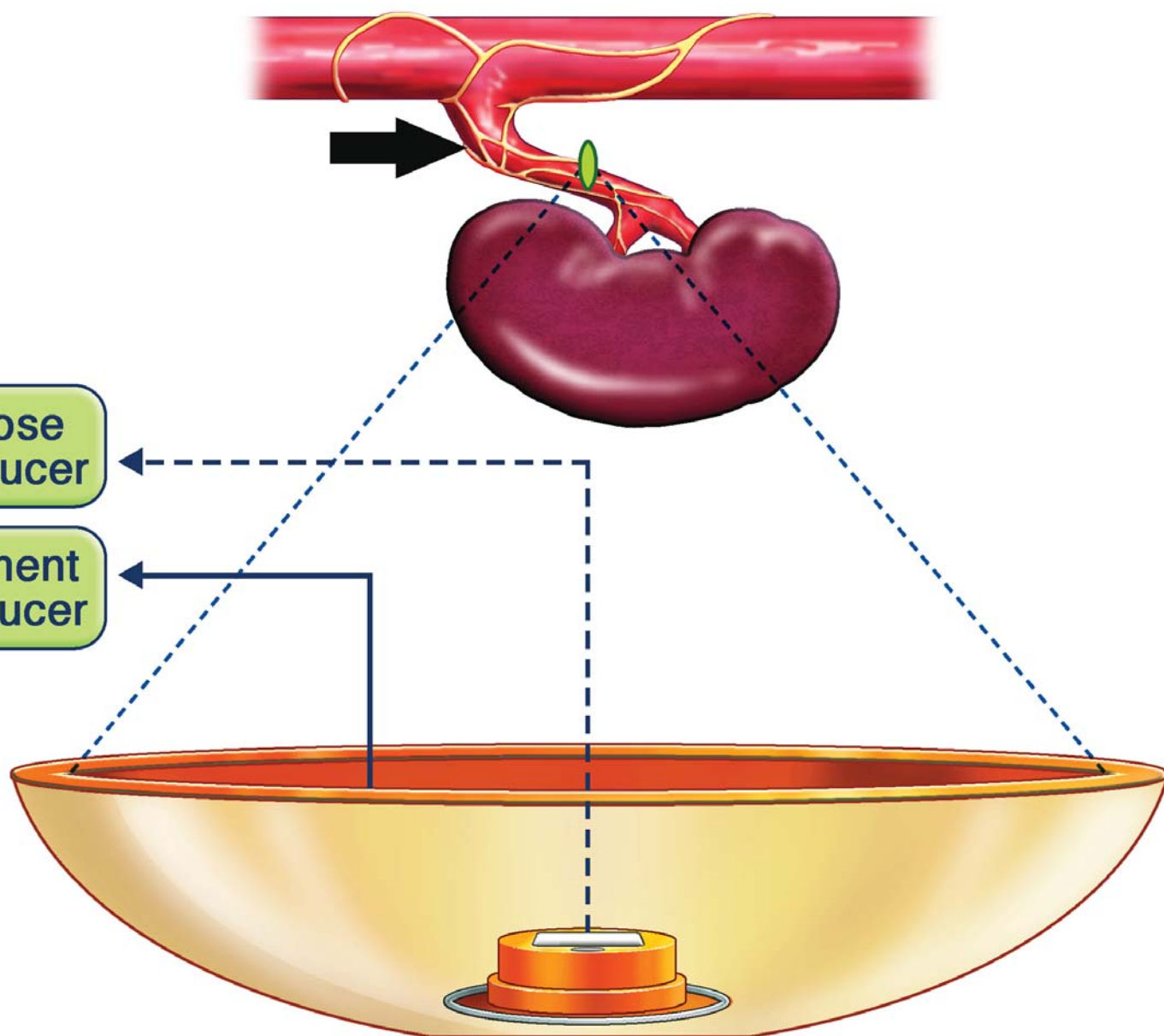
- The myxoid change in the appearance of the nerve fibers was more distinct on day 28 than on day 6.

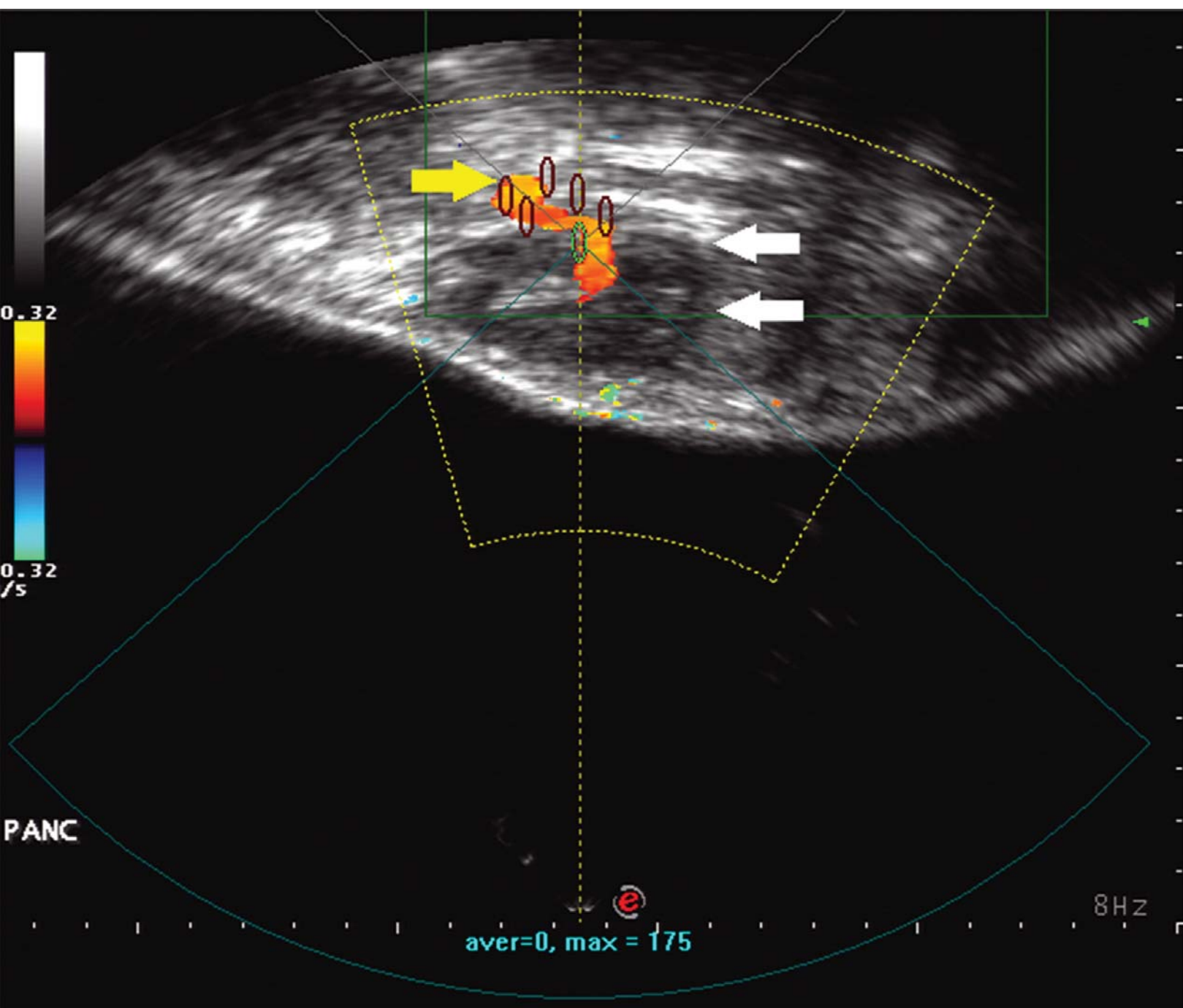
Table 1. BP, NA and renal function of the ablation and sham group on baseline, days 6 and 28

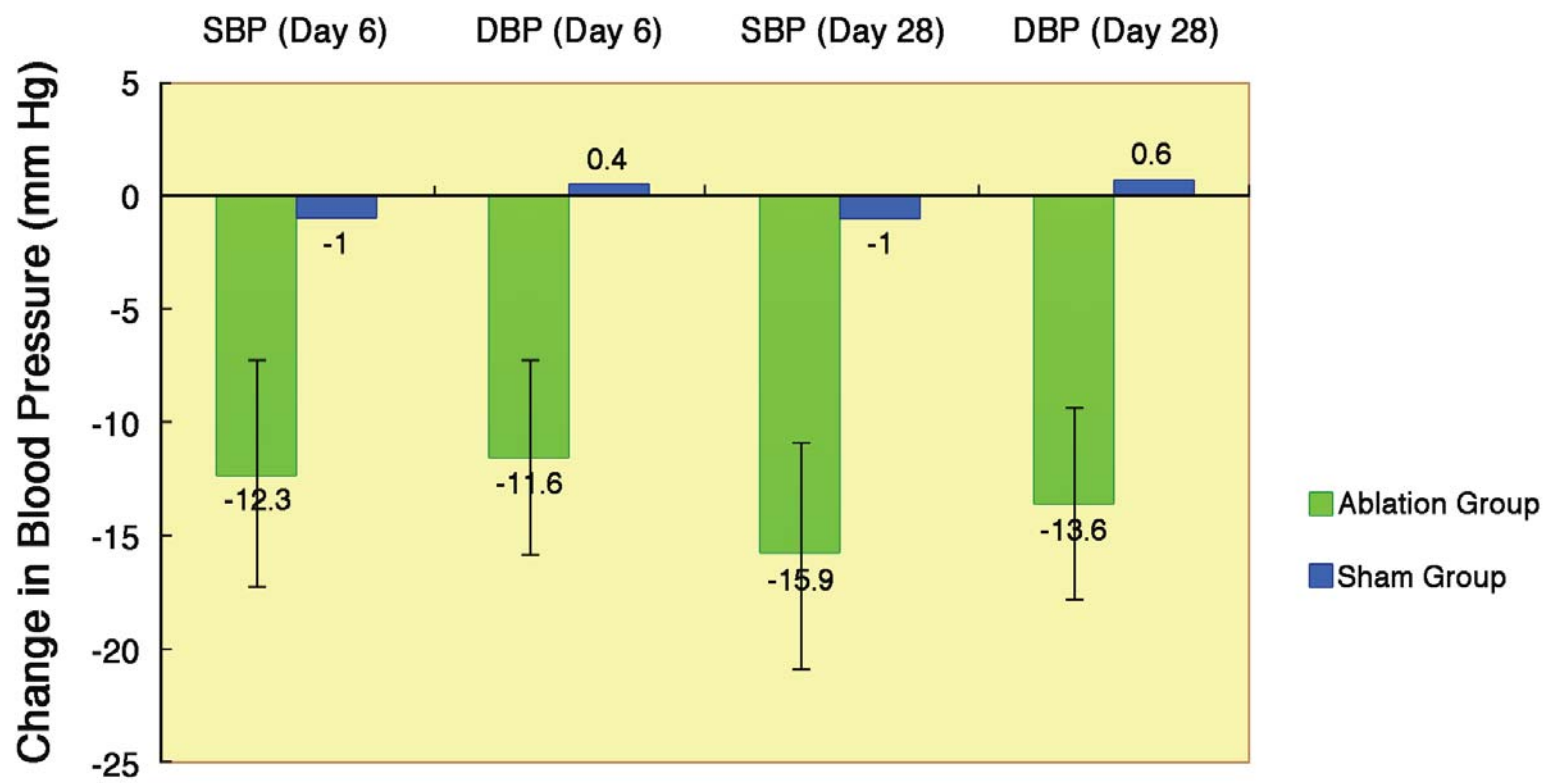
Ablation Group (N=18)												
	Euthanatized at day 6			Euthanatized at day			Sham Group (N=5)					
	(N=10)			28(N=8)								
	Baseline	Day 6	p*	Baseline	Day 28	p*	Baseline	Day 6	p†	Day 28	p‡	p§
SB	124.1(7.3)	111.8(7.5)	<0.001	128.8(9.4)	112.9(8.4)	<0.001	125.8(8.3)	126.2(8.6)	0.002	126.4(7.7)	0.011	0.987
P			1			1						
DB	82.0(9.1)	70.4(7.8)	<0.001	83.1(10.1)	69.5(7.4)	<0.001	82.4(7.3)	82.2(8.3)	0.015	83.0(8.4)	0.011	0.957
P			1			1						
NA	582.9(82.3)	290.0(41.1)	<0.001	587.3(79.5)	261.8(67.0)	<0.001	596.8(84.1)	564.8(80.4)	<0.001	545.4(97.9)	<0.001	0.423
Na ⁺	149.7(4.2)	148.3(4.0)	0.417	149.3(5.3)	142.6(3.1)	0.007	149.9(4.5)	150.4(3.7)	0.359	149.3(4.5)	0.014	0.940
BU	3.63(0.4)	3.38(0.6)	0.180	3.68(0.5)	3.48(0.7)	0.537	3.54(0.36)	3.62(0.8)	0.482	3.90(1.2)	0.327	0.769
N												
sCr	54.9(8.3)	53.9(7.7)	0.637	53.6(4.7)	52.3(3.7)	0.763	53.4(7.5)	59.1(5.5)	0.217	58.0(14.1)	0.196	0.660

Values are mean (SD). *Post ablation vs. baseline. † Ablation group vs. sham group at day 6.

‡Ablation group vs. sham group at day 28. §Within-group comparisons for the sham group.







Change% in NA and Renal Function
on Day 6 and 28